



## Case report

# Utility of nerve ultrasound in the management of primary neurolymphomatosis: Case report and review of the literature



Arena Wada <sup>a</sup>, Yudai Uchida <sup>a</sup>, Keiichi Hokkoku <sup>a,\*</sup>, Amuro Kondo <sup>a</sup>, Yuki Fujii <sup>a</sup>, Takashi Chiba <sup>a</sup>, Takuji Matsuo <sup>b</sup>, Hiroshi Tsukamoto <sup>c</sup>, Yuki Hatanaka <sup>a</sup>, Shunsuke Kobayashi <sup>a</sup>, Masahiro Sonoo <sup>a</sup>

<sup>a</sup> Department of Neurology, Teikyo University School of Medicine, Tokyo 173-8606, Japan

<sup>b</sup> Department of Hematology, Teikyo University School of Medicine, Tokyo 173-8606, Japan

<sup>c</sup> Kensei Clinic, Ibaraki 309-1211, Japan

## ARTICLE INFO

## Article history:

Received 6 February 2023

Received in revised form 8 April 2023

Accepted 16 April 2023

Available online 6 May 2023

## Keywords:

Neurolymphomatosis

Primary neurolymphomatosis

Imaging study

Ultrasound

Ultrasonography

## ABSTRACT

**Introduction:** Primary neurolymphomatosis (NL) is a critical differential diagnosis of asymmetric multiple mononeuropathy and radiculoplexopathy. Its diagnosis is often challenging due to the lack of typical clinical signs of systemic lymphoma. We report a case of primary NL where nerve ultrasound (NUS) played an important role in the diagnosis and follow-up of the disease.

**Case presentation:** A 52-year-old man developed asymmetric painful multiple mononeuropathy in the right upper limb with cranial nerve involvement. After being referred to our department, the patient underwent NUS, which revealed marked enlargement and increased vascularity in the right upper limb nerves, brachial plexus, and cervical nerve roots. Furthermore, an epineural hypoechoic mass, a characteristic finding of NL, was seen in the right median nerve. These NUS findings prompted us to perform 18F-fluorodeoxyglucose positron emission tomography/computed tomography and a subsequent biopsy on the right axillary lymph node, confirming NL. Notably, the NUS abnormalities dramatically subsided, demonstrating the effectiveness of chemotherapy.

**Discussion:** The diagnostic utility of NUS for NL has been documented by many recent reports. Additionally, NUS can work as a quick follow-up tool for NL, as seen in our case.

© 2023 International Federation of Clinical Neurophysiology. Published by Elsevier B.V. This is an open access article under the CC BY-NC-ND license (<http://creativecommons.org/licenses/by-nc-nd/4.0/>).

## 1. Introduction

Neurolymphomatosis (NL) is a rare complication of non-Hodgkin lymphoma (NHL) and leukemia, where tumor cells directly infiltrate the peripheral nervous system (Tomita et al. 2013; Del Grande et al. 2014; Vijayan et al. 2015; Tai et al. 2019). It often demonstrates subacute asymmetric motor weakness and sensory disturbance, manifesting multiple mononeuropathy, radiculopathy, or plexopathy with a varying degree of neuropathic pain (Tomita et al. 2013; Del Grande et al. 2014; Gwathmey 2018). More rarely, NL can be the initial manifestation of NHL and leukemia, designated as primary NL (Wai et al. 2012;

Del Grande et al. 2014; Campagnolo et al. 2020). Several reports have documented its diagnostic difficulty due to the absence of clinical signs of systemic lymphoma and misleading neurological features mimicking other neurological diseases (Tomita et al. 2013; Del Grande et al. 2014; Gwathmey 2018).

Nerve ultrasound (NUS), with its high resolution and non-invasiveness, has become a common tool for evaluating the peripheral nervous system. Several authors have recently highlighted the utility of NUS in diagnosing NL (Vijayan et al. 2015; Walker and Cartwright 2015). Nevertheless, its practical use is still under development. Herein, we report a case of primary NL in which NUS played an important role in the diagnosis and follow-up of the disease. We also discuss how NUS can be integrated with other major examinations for NL, such as nerve conduction studies (NCS), magnetic resonance imaging (MRI), and fluorine-18 fluorodeoxyglucose positron emission tomography/computed tomography (18F-FDG PET/CT) based on a literature review. The present study was conducted in accordance with the guidelines of the Declaration of Helsinki. Informed consent was obtained from all patients for this report.

\* Corresponding author at: Department of Neurology, Teikyo University School of Medicine, Kaga 2-11-1, Itabashi-Ku, Tokyo 1738606, Japan.

E-mail addresses: [y-uchida@med.teikyo-u.ac.jp](mailto:y-uchida@med.teikyo-u.ac.jp) (Y. Uchida), [k1-hokkoku@hotmail.co.jp](mailto:k1-hokkoku@hotmail.co.jp) (K. Hokkoku), [tk-chiba@med.teikyo-u.ac.jp](mailto:tk-chiba@med.teikyo-u.ac.jp) (T. Chiba), [matsuo-taku2@med.teikyo-u.ac.jp](mailto:matsuo-taku2@med.teikyo-u.ac.jp) (T. Matsuo), [y-hata@med.teikyo-u.ac.jp](mailto:y-hata@med.teikyo-u.ac.jp) (Y. Hatanaka), [sonoom@med.teikyo-u.ac.jp](mailto:sonoom@med.teikyo-u.ac.jp) (M. Sonoo).

## 2. Case presentation

A 52-year-old man developed right facial paralysis in 2018, but the symptom subsided with corticosteroids. Two years later, the patient experienced numbness from the face to the neck on the left side. In February 2022, he started to feel persistent pain and numbness in his right hand. He could not raise his right upper limb four months later, bringing him to the previous hospital. Because of the asymmetric clinical symptoms, suggesting multiple mononeuropathies, and the lack of particular clinical and laboratory findings in other organs, non-systemic vasculitic neuropathy (NSVN) was initially suspected. Chronic inflammatory demyelinating polyradiculoneuropathy (CIDP) was also suspected based on the hypertrophy of the right brachial plexus observed on MRI, although NCS suggested axonal neuropathy. Two courses of intravenous methylprednisolone (1,000 mg for three days) and one course of intravenous injection of immunoglobulin (0.4 g/[kg/day]) were administered but failed to improve his symptoms. Despite the medication, his right upper limb symptoms gradually deteriorated over the following months, and the right facial paralysis returned.

In July 2022, the patient was referred to our hospital for further investigation. Physical examination revealed right facial paralysis and diffuse right upper limb weakness (Medical Research Council grade 0–1/5, grip strength was not measurable) with severe muscle atrophy and areflexia. The weakness and atrophy were distributed from the C5 muscles, like the deltoid and biceps brachii muscles, to the C8/T1 muscles, like the thenar, hypothenar, interosseus, and lumbrical muscles. Severe dysesthesia and hypoesthesia were observed in the right upper limb. In addition, mild dysesthesia was seen in the left face and anterior part of the neck. Blood tests revealed negative vasculitis-associated immune markers, including antinuclear and antineutrophil cytoplasmic antibodies. Meanwhile, soluble interleukin-2 receptor (sIL-2R) was elevated (1,198 U/ml). Cerebrospinal fluid (CSF) analysis showed slightly increased blood cells (14 / $\mu$ L), but the protein level remained normal. A set of conventional NCS showed absent compound muscle action potentials (CMAP) and sensory nerve action potentials (SNAP) in the right median and ulnar nerves. The right axillary nerve showed

markedly decreased CMAP amplitude of the deltoid muscle. Meanwhile, no abnormalities were found in the right lower limb. Together with the severe muscle atrophy, the absent or diminished CMAP indicated that the main pathophysiology of the patient was axonal degeneration. Additionally, the loss of SNAP suggested that postganglionic segments (i.e., the peripheral nerves, brachial plexus, or both areas) were involved. The results of NCS conducted at the time of admission are summarized in Table 1. We did not perform needle electromyography, considering the marked abnormalities in the NCS and the invasiveness to the patient. NUS was performed as the first imaging study using an 18 MHz linear array probe. The right median nerve showed marked enlargement with swollen nerve fascicles and perineurium. Additionally, a fusiform hypochoic mass was observed between the nerve and the thickened epineurium (Fig. 1A, Supplementary Video 1). These findings were compatible with those reported in past NL cases (Choi et al. 2008; Wai et al. 2012; Vijayan et al. 2015; Tai et al. 2019; Yaseen et al. 2019; Lee et al. 2020; Lee et al. 2021). The right ulnar and musculocutaneous nerves also showed segmental enlargement with loss of normal fascicular pattern. Furthermore, massive enlargement with increased vascularity in the perineurium and epineurium was observed in the right nerve roots and brachial plexus (Fig. 1B, Supplementary Video 2). Subsequent MRI revealed massive swelling of the right median nerve, nerve roots, and brachial plexus, consistent with the NUS findings, and these structures showed abnormal FDG uptake on 18F-FDG PET/CT, suggesting NL (Fig. 1D–F). These imaging studies also revealed a right axillary lymph node lesion, later biopsied and confirmed as diffuse large B-cell lymphoma (DLBCL). The patient was finally diagnosed with NL and was moved to the hematology unit on August 6, 2022 to receive chemotherapy.

One month later, the first two courses of chemotherapy had relieved his neuropathic pain, unlike immunotherapy (i.e., intravenous methylprednisolone and immunoglobulin), which showed no effect on his symptoms. However, severe muscle weakness and sensory disturbance remained. CMAP and SNAP in NCS were still absent, suggesting severe axonal loss and poor functional outcome (Table 1, Post-chemotherapy). Nevertheless, in the NUS, the

Table 1

On admission	MCS	Nerve	Distal latency (ms)	Amplitudes (mV)	CV (m/s)
		Median	–	<u>Not evoked</u>	–
		Ulnar	–	<u>Not evoked</u>	–
		Tibial	12.4	Ankle: 29.2 Knee: 21.7	46
		Peroneal	14.7	Ankle 6.9 Below knee 6.3 Above knee 5.4	40 47
		Axillary (Deltoid)	2.4	<u>0.35</u>	
	F-study	Nerve	F-wave latency (ms)		CV (m/s)
		Median	–		–
		Ulnar	–		–
		Tibial	45.5		56
	SCS	Nerve	Distal latency (ms)	Amplitudes ( $\mu$ V)	CV (m/s)
		Median	–	<u>Not evoked</u>	–
		Ulnar	–	<u>Not evoked</u>	–
		Sural	3.4	26.4	56
Post-chemotherapy	MCS	Nerve	Distal latency (ms)	Amplitudes (mV)	CV (m/s)
		Median	–	<u>Not evoked</u>	–
		Ulnar	–	<u>Not evoked</u>	–
		Axillary (Deltoid)	–	<u>Not evoked</u>	–
	SCS	Nerve	Distal latency (ms)	Amplitudes ( $\mu$ V)	CV (m/s)
		Median	–	<u>Not evoked</u>	–
		Ulnar	–	<u>Not evoked</u>	–

Abnormal findings are underlined according to our laboratory's established reference values. CV: conduction velocity, MCS: motor nerve conduction study, SCS: sensory nerve conduction study.

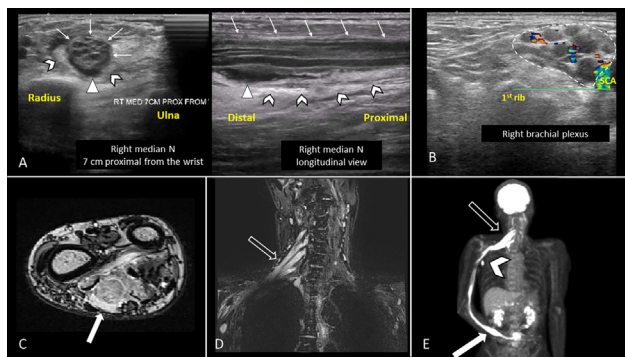


**Fig. 1.** NUS, MRI, and 18F-FDG PET/CT findings. A: NUS of the right median nerve shows marked enlargement (CSA: 54 mm<sup>2</sup>) at the forearm, 7 cm proximal from the wrist in short-axis and longitudinal views (thin arrows). The nerve fascicles and perineurium are swollen, resulting in irregular fascicular patterns. A fusiform hypoechoic mass (triangles) is observed between the nerve and thickened epineurium (arrowheads). B: NUS shows massive enlargements of the supraclavicular region of the brachial plexus (dotted frame) (167 mm<sup>2</sup>). Color Doppler imaging depicts increased epineural and perineural vascularity. C: A Dixon sequence of MRI shows the enlarged right median nerve with a short-axis view. The nerve is surrounded by the thickened epineurium, consistent with the NUS findings (white arrow). D: Massive enlargement of the right nerve roots and brachial plexus is seen in MRI with a STIR sequence (open arrow). E: 18F-FDG PET/CT shows an abnormal FDG uptake in the right median nerve (white arrows), nerve roots, and brachial plexus (open arrows), corresponding to the abnormal findings in the NUS and MRI. The right axillary lymph node also shows abnormal uptake (arrowhead). \* Normal values for CSA at our laboratory for the evaluated sections: the median nerve (wrist), 8 mm<sup>2</sup>; the brachial plexus, 45 mm<sup>2</sup>. CSA, cross-sectional area; MRI, magnetic resonance imaging; NUS, nerve ultrasound; SCA, subclavian artery; 18F-FDG PET/CT, fluorine-18 fluorodeoxyglucose positron emission tomography/computed tomography.

enlargement of the nerves, brachial plexus, and nerve roots had dramatically subsided, demonstrating the effectiveness of chemotherapy (Fig. 2).

### 3. Discussion

Delayed diagnosis is relatively common in primary NL due to the lack of specific clinical and laboratory findings (Tomita et al. 2013; Del Grande et al. 2014). The most commonly reported clinical phenotype of NL is multiple mononeuropathy/plexopathy/radiculopathy with possible cranial nerve involvement, usually accompanied by varying degrees of neuropathic pain, as seen in our case (Grisariu et al. 2010). While asymmetric distribution can be the clue for diagnosing NL, several neuropathies should be carefully ruled out. In light of the present case, NSVN, which typically

manifests painful multiple mononeuropathies and multifocal CIDP, previously known as “MADSAM”, can be the crucial differential diagnosis (Tomita et al. 2013; Briani et al. 2019; Keddie et al. 2020; Jeong et al. 2021). When ruling out NSVN, cranial nerve involvement may be helpful as it is more commonly seen in NL (20–46%) than NSVN (6%) (Grisariu et al. 2010; Tomita et al. 2013; Collins et al. 2019; Keddie et al. 2020; Jeong et al. 2021). Meanwhile, it should be noted that cranial nerve involvement is seen in up to 48% of multifocal CIDP (Shibuya et al. 2020). In this setting, neuropathic pain can be the sign to exclude multifocal CIDP. While most NL patients (80–100%) show neuropathic pain due to lymphoma cell infiltration, this symptom is rarely seen in CIDP (7%) (Nasu et al. 2012; Tomita et al. 2013; Keddie et al. 2020; Jeong et al. 2021). In the present case, the combination of asymmetric neurological deficits, cranial nerve involvement, and neuropathic pain suggested NL rather than NSVN or multifocal CIDP.

With regard to laboratory tests, the results should also be carefully assessed in NL. In NCS, for example, the disease typically shows axonal degeneration, but the findings are not disease-specific, and some cases even show demyelinating findings mimicking CIDP (Tomita et al. 2013; Del Grande et al. 2014; Kamiya-Matsuoka et al. 2014; Campagnolo et al. 2020). Additionally, conventional blood markers, such as serum sIL-2R level, lack sufficient accuracy (Tomita et al. 2013). In this context, imaging studies, including NUS, MRI, and 18F-FDG PET/CT, play an important role in the further evaluation of NL.

In the present case, although the final diagnosis of NL was made by 18F-FDG PET/CT and a subsequent biopsy of the axillary lymph nodes, NUS worked as a quick tool to reveal morphological changes in the peripheral nervous system caused by NL. Furthermore, follow-up NUS assessment demonstrated the effectiveness of chemotherapy through chronological changes in the nerve structures. To address the utility of NUS for the management of NL, a publication search was performed on PubMed, Web of Science, Scopus, and Google Scholar using the keywords “neurolymphomatosis”, “ultrasound”, and “ultrasonography” (the search was conducted on December 18, 2022). We identified 17 cases with NL in which NUS was performed during their disease course from 12 case reports and two case series (Choi et al. 2008; von Falck et al. 2009; Wai et al. 2012; Hanna et al. 2013; Del Grande et al. 2014; Vijayan et al. 2015; Briani et al. 2017; Yaseen et al. 2019; Iacobellis et al. 2019; Tai et al. 2019; Campagnolo et al. 2020; Lee et al. 2020; Lee et al. 2021; Fargeot et al. 2021). To the best of our knowledge, six of these have never been cited anywhere else (Wai et al. 2012; Iacobellis et al. 2019; Yaseen et al. 2019; Lee et al. 2020; Lee et al. 2021; Fargeot et al. 2021). The details of the reported cases and the present case, a total of 18 cases, are described in Table 2. Most cases showed nerve enlargement (89%, 16/18 cases) and an abnormal fascicular pattern (81%, 13/16 cases) originating from diffuse swelling of nerve fascicles and perineurium. In these cases, the normal fascicular structure was merely observed, and the nerve became markedly hypoechoic, as seen in our case. Infiltration of lymphoma cells was confirmed in all cases where a biopsy was performed on the nerve with the abnormal NUS findings (eight cases). In addition, if it was evaluated, increased vascularity was frequently observed in doppler assessments (90%, 9/10 cases). Tumor-associated angiogenesis has been postulated as a possible cause of this phenomenon (Vijayan et al. 2015). In the present case, an epineural hypoechoic lesion was another characteristic finding. This particular finding was found in nine cases in the past literature (Choi et al. 2008; Wai et al. 2012; Vijayan et al. 2015; Yaseen et al. 2019; Lee et al. 2020; Lee et al. 2021). Its frequency reached 63% (10/16 cases), including ours. In these cases, the nerve fascicles, either with or without enlargement, were surrounded by a segmental

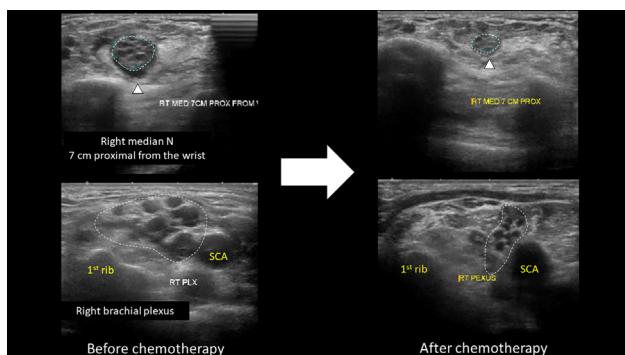


**Fig. 2.** Sequential NUS assessments. The CSA of the right median nerve at the forearm and the brachial plexus (supraclavicular region) shows a remarkable decrease after two courses of chemotherapy (54 mm<sup>2</sup> to 16 mm<sup>2</sup> and 167 mm<sup>2</sup> to 63 mm<sup>2</sup>, respectively). CSA, cross-sectional area; SCA, subclavian artery.

Table 2

Author	N	Primary or secondary	Lymphoma type	Neuropathy phenotype	NUS findings					Abnormalities of other modalities corresponding to NUS findings			
					Examined nerve	Nerve enlargement	Abnormal fascicular pattern	Increased vascularity (doppler)	Epineural hypoechoic lesion	MRI	FDG PET	NCS	Biopsy
Choi et al. 2008	1	secondary	DLBCL	MN	ulnar N	(+)	(+)	(+)	(+)	(+)	(+)	N.A	(+)
Von Falck et al. 2009	1	primary	DLBCL	PN	median N (axilla)	(+)	N.A	N.A	N.A	(+)	(+)	N.A	N.A
Hanna et al. 2013	1	secondary	mycosis fungoides	multiple MN	ulnar N	(+)	(+)	(–)	(–)	N.A	N.A	(+)	(+)
Wai et al. 2012	2	secondary	DLBCL	multiple MN	median N	(+)	(+)	N.A	(+)	(+)	(+)	N.A	N.A
Del Grande et al. 2014	1	secondary	DLBCL	multiple MN	tibial N	(+)	(+)	N.A	(+)	(+)	(+)	N.A	(+)*
Vijayan et al. 2015	1	primary	DLBCL	multiple MN	radial N, femoral N, brachial plexus, cervical nerve roots	(+)	(+)	N.A	(–)	N.A	(+)	(+)	(+)
Briani et al. 2017	3	secondary	DLBCL	MN	median N	(+)	(+)	(+)	(–)	(+)	(+)	(+)	(+)
		secondary	T-cell	MN	ulnar N	(+)	(+)	(+)	(–)	(+)	N.A	(+)	(+)
		secondary	DLBCL	MN	sciatic N	(+)	(+)	(+)	(+)	(+)	N.A	(+)	(+)
Iacobellis et al. 2019	1	primary	CLL	MN	tibial N	(–)	(–)	(+)	(–)	N.A	N.A	(+)	N.A
Tai et al. 2019	1	secondary	MALT	MN	radial N	(+)	(+)	(+)	(+)	(+)	(+)	N.A	N.A
Yaseen et al. 2019	1	secondary	Burkitt-like	MN	median N	(+)	(+)	(+)	(+)	N.A	(+)	N.A	(+)
Lee et al. 2020	1	secondary	DLBCL	MN	sciatic N, tibial N, fibular N	(+)	N.A	N.A	(+)	(+)	(+)	N.A	(+)
Campagnolo et al. 2020	1	secondary	DLBCL	MN	sciatic N	(+)	(+)	N.A	(+)	N.A	(+)	(+)	N.A
Fargeot et al. 2021	1	secondary	DLBCL	multiple RP	median N, radial N, ulnar N, brachial plexus, sciatic N, fibular N, tibial N, sural N	(–)	(–)	N.A	N.A	(–)	(–)	N.A	N.A
Lee et al. 2021	1	secondary	Subcutaneous B-cell	MN	superficial fibular N	(+)	(+)	N.A	(–)	(+)	N.A	(+)	(+)
Present case	1	primary	DLBCL	MN	sciatic N, tibial N	(+)	(–)	(+)	(+)	N.A	(+)	N.A	(+)*
	1	primary	DLBCL	multiple MN	median N, radial N, ulnar N, musculocutaneous N, brachial plexus, cervical nerve roots	(+)	(+)	(+)	(+)	(+)	(+)	(+)	N.A

CLL, chronic lymphocytic leukemia; DLBCL, diffuse large B-cell lymphoma; FDG PET, <sup>18</sup>F fluorodeoxyglucose positron emission tomography/computed tomography. M.N. mononeuropathy; MRI, magnetic resonance imaging; N, nerve; N.A; not assessed; NCS, nerve conduction study; NUS; nerve ultrasound; P.N., polyneuropathy; R.P., radiculoplexopathy. \* biopsy on an epineural mass.

fusiform epineural hypoechoic mass. This finding has been documented as a “fried egg sign”, describing the contrast of hypo- and hyper-echogenicity originating from the epineural mass and the nerve fascicles (Lee et al. 2021). In two cases, needle biopsy confirmed lymphoma cells from the epineural mass, suggesting an association between the abundant lymphatic flow in the epineurium and tumor infiltration (Wai et al. 2012; Lee et al. 2021). While an epineural hypoechoic lesion may be a less frequent finding than nerve enlargement and increased vascularity, it can be a more pathognomonic finding of NL. It is known that nerve enlargement and increased vascularity are commonly seen in immune-mediated neuropathies, including vasculitic neuropathy and CIDP, whereas an epineural lesion is rarely seen in these diseases (Padua et al. 2013; Goedee et al. 2014). In the present case, the epineural hypoechoic lesion prompted us to perform 18F-FDG PET/CT to confirm NL.

Regarding the abnormalities in NUS and other diagnostic modalities, strong relationships were observed among them in the reported NL cases and the present case. Specifically, if NUS showed the abovementioned abnormalities, MRI, 18F-FDG PET/CT, NCS, and biopsy were likely to show positive findings. Considering its accessibility, NUS can be used as the first imaging modality in NL.

Notably, our case demonstrates the utility of NUS in evaluating the effectiveness of chemotherapy by morphological improvement of the nerve structures. NCS is a common tool for evaluating neuropathy. However, NL usually causes irreversible axonal degeneration, and CMAP and SNAP are sometimes absent, leading to the difficulty of NCS assessments (Campagnolo et al. 2020). Although the utility of MRI and 18F-FDG PET/CT for assessing chemotherapy effectiveness has been reported (Iacobellis et al. 2019), their availability tends to be limited, and sequential studies are not always feasible. Hence, the complementary use of NUS may allow for a quick, objective assessment of chemotherapy effectiveness in NL.

In conclusion, NUS works as a quick imaging study to reveal NL and may have a strong relationship with abnormalities found in other laboratory tests. In addition, NUS can be used as a follow-up tool for NL by sequentially evaluating morphological changes in the nerves.

## Declaration of Competing Interest

The authors declare that they have no known competing financial interests or personal relationships that could have appeared to influence the work reported in this paper.

## Appendix A. Supplementary material

Supplementary material to this article can be found online at <https://doi.org/10.1016/j.cnp.2023.04.003>.

## References

- Briani, C., Visentin, A., Cavallaro, T., Cacciavillani, M., Cabrini, I., Ferrari, S., et al., 2017. Primary neurolymphomatosis as clinical onset of chronic lymphocytic leukemia. *Ann. Hematol.* 96 (1), 159–161. <https://doi.org/10.1007/s00277-016-2852-2>.
- Briani, C., Visentin, A., Campagnolo, M., Salvalaggio, A., Ferrari, S., Cavallaro, T., et al., 2019. Peripheral nervous system involvement in lymphomas. *J. Peripher. Nerv. Syst.* 24 (1), 5–18.
- Campagnolo, M., Cacciavillani, M., Cavallaro, T., Ferrari, S., Gasparotti, R., Zambello, R., et al., 2020. Neurolymphomatosis, a rare manifestation of peripheral nerve involvement in lymphomas: Suggestive features and diagnostic challenges. *J. Peripher. Nerv. Syst.* 25 (3), 312–315.

- Choi, A.L., Sung, H.K., Sun, Y.J., Hee, S.H., Hye, W.C., Kyung, M.J., et al., 2008. Lymphoma involving the ulnar nerve: Sonographic findings. *J. Ultrasound Med.* 27 (10), 1527–1531.
- Collins, M.P., Dyck, P.J.B., Hadden, R.D.M., 2019. Update on classification, epidemiology, clinical phenotype and imaging of the non-systemic vasculitic neuropathies. *Curr. Opin. Neurol.* 32 (5), 684–695.
- Del Grande, A., Sabatelli, M., Luigetti, M., Conte, A., Granata, G., Rufini, V., et al., 2014. Primary multifocal lymphoma of peripheral nervous system: Case report and review of the literature. *Muscle Nerve* 50 (6), 1016–1022.
- Fargeot, G., Maisonobe, T., Vandendries, C., Le Garff-Tavernier, M., Leblond, V., Viala, K., 2021. Neurolymphomatosis related to direct epineural invasion of the superficial peroneal nerve from subcutaneous B-cell lymphoma. *Clin. Neurol. Neurosurg.* 210. <https://doi.org/10.1016/j.clineuro.2021.106992>.
- Goedee, H.S., Brekelmans, G.J.F., Visser, L.H., 2014. Multifocal enlargement and increased vascularization of peripheral nerves detected by sonography in CIDP: A pilot study. *Clin. Neurophysiol.* 125 (1), 154–159. <https://doi.org/10.1016/j.clinph.2013.05.025>.
- Grisariu, S., Avni, B., Batchelor, T.T., Van Den Bent, M.J., Bokstein, F., Schiff, D., et al., 2010. Neurolymphomatosis: An International Primary CNS Lymphoma Collaborative Group report. *Blood* 115 (24), 5005–5011.
- Gwathmey KG. Plexus and peripheral nerve metastasis. 1st ed. Vol. 149, *Handbook of Clinical Neurology*. Elsevier B.V.; 2018. <https://doi.org/10.1016/B978-0-12-811161-1.00017-7>.
- Hanna, R., Di Primio, G.A., Schweitzer, M., Torres, C., Sheikh, A., Chakraborty, S., 2013. Progressive neurolymphomatosis with cutaneous disease: Response in a patient with mycosis fungoides. *Skeletal Radiol.* 42 (7), 1011–1015.
- Iacobellis, F., Di Serafino, M., Blasio, R., Barbuto, L., Pezzullo, F., Romano, L., 2019. Secondary neurolymphomatosis of the radial nerve: A diagnostic challenge. *Am. J. Case Rep.* 20, 1652–1658.
- Jeong, J., Kim, S.W., Sung, D.H., 2021. Neurolymphomatosis: a single-center experience of neuromuscular manifestations, treatments, and outcomes. *J. Neurol.* 268 (3), 851–859. <https://doi.org/10.1007/s00415-020-10202-0>.
- Kamiya-Matsuoka, C., Shroff, S., Gildersleeve, K., Hormozdi, B., Manning, J.T., Woodman, K.H., 2014. Neurolymphomatosis: A case series of clinical manifestations, treatments, and outcomes. *J. Neurol. Sci.* 343 (1–2), 144–148. <https://doi.org/10.1016/j.jns.2014.05.058>.
- Keddie, S., Nagendran, A., Cox, T., Bomsztyk, J., Jaunmuktane, Z., Brandner, S., et al., 2020. Peripheral nerve neurolymphomatosis: Clinical features, treatment, and outcomes. *Muscle Nerve* 62 (5), 617–625.
- Lee, C.Y., Ho, T.Y., Wu, Y.T., Chen, L.C., Lee, T.Y., 2020. Recurrent diffuse large B-cell lymphoma involving the sciatic nerve: A rare case report and review of the literature. *J. Med. Sci.* 40 (5), 236–240.
- Lee, Y.C., Huang, G.S., Chang, W.C., Hsu, Y.C., 2021. Fried egg sign: A typical ultrasonography feature of neurolymphomatosis. *J. Clin. Ultrasound* 49 (8), 878–880.
- Nasu, S., Misawa, S., Sekiguchi, Y., Shibuya, K., Kanai, K., Fujimaki, Y., et al., 2012. Different neurological and physiological profiles in POEMS syndrome and chronic inflammatory demyelinating polyneuropathy. *J. Neurol. Neurosurg. Psychiatry* 83 (5), 476–479.
- Padua, L., Paolasso, I., Pazzaglia, C., Granata, G., Lucchetta, M., Erra, C., et al., 2013. High ultrasound variability in chronic immune-mediated neuropathies. Review of the literature and personal observations. *Rev. Neurol. (Paris)* 169 (12), 984–990. <https://doi.org/10.1016/j.neuro.2013.07.028>.
- Shibuya, K., Tsuneyama, A., Misawa, S., Suichi, T., Suzuki, Y., Kojima, Y., et al., 2020. Cranial nerve involvement in typical and atypical chronic inflammatory demyelinating polyneuropathies. *Eur. J. Neurol.* 27 (12), 2658–2661.
- Tai, R., Maingard, J., Nambiar, M., Lim, K., 2019. High-grade B-cell lymphoma relapse presenting as neurolymphomatosis of the median nerve. *BMJ Case Rep.* 12 (3), 2018–2020.
- Tomita, M., Koike, H., Kawagashira, Y., Iijima, M., Adachi, H., Taguchi, J., et al., 2013. Clinicopathological features of neuropathy associated with lymphoma. *Brain* 136 (8), 2563–2578.
- Vijayan, J., Chan, Y.C., Therimadasamy, A., Wilder-Smith, E.P., 2015. Role of combined B-mode and Doppler sonography in evaluating neurolymphomatosis. *Neurology* 85 (9), 752–755.
- von Falck, C., Rodt, T., Joerdens, S., Waldeck, S., Kiesel, H., Knapp, W.H., et al., 2009. F-18 2-fluoro-2-deoxy-glucose positron emission tomography/computed tomography for the detection of radicular and peripheral neurolymphomatosis: Correlation with magnetic resonance imaging and ultrasound. *Clin. Nucl. Med.* 34 (8), 493–495.
- Wai, J.W.C., Chan, M.K., Tang, K.W., Chan, S.C.H., 2012. Neurogenic tumour mimicker: Two cases of neurolymphomatosis. *Hong Kong J. Radiol.* 15 (3), 187–191.
- Walker, F.O., Cartwright, M.S., 2015. Ultrasound in neurolymphomatosis: The rise of the machines. *Neurology* 85 (9), 746–747.
- Yaseen, M.T., Aziz, P.A.A., Siddique, K., Tariq, T.A., 2019. Neurolymphomatosis of the sciatic and tibial nerves. *J. Coll. Physicians Surg. Pakistan* 29 (Supplement 2), S86–S88.